THE MORPHOLOGY OF PASSIVELY EVOLVING GALAXIES AT $Z \sim 2$ FROM *HST*/WFC3 DEEP IMAGING IN THE HUBBLE ULTRADEEP FIELD[1]

P. CASSATA[2], M. GIAVALISCO[2], YICHENG GUO[2], H. FERGUSON[3], A. KOEKEMOER[3], A. RENZINI[4], A. FONTANA[5], S. SALIMBENI[2], M. DICKINSON[6], S. CASERTANO[3], C. J. CONSELICE[7], N. GROGIN[3], J. M. LOTZ[6], C. PAPOVICH[8], R. A. LUCAS[3], A. STRAUGHN[9], J. P. GARDNER[9], L. MOUSTAKAS[10]

Draft version November 13, 2009

ABSTRACT

We present near–IR images of six passive galaxies (SSFR$< 10^{-2}$ Gyr^{-1}) at redshift $1.3 < z < 2.4$ with stellar mass $M \sim 10^{11}$ M$_\odot$, selected from the Great Observatories Origins Deep Survey (GOODS), obtained with the *Hubble Space Telescope* (*HST*) and the WFC3/IR camera. These images provide the deepest and highest angular resolution view of the optical rest–frame morphology of such systems to date. We find that the light profile of these galaxies is generally regular and well described by a Sérsic model with index typical of today's spheroids. We confirm the existence of compact and massive early–type galaxies at $z \sim 2$: four out of six galaxies have $r_e \sim 1$ kpc or less. The images reach limiting surface brightness $\mu \sim$26.5 mag arcsec^{-2} in the F160W bandpass; yet there is no evidence of a faint halo in the galaxies of our sample, even in their stacked image. We also find very weak "morphological k–correction" in the galaxies between the rest–frame UV (from the ACS z–band), and the rest–frame optical (WFC3 H–band): the visual classification, Sérsic indices and physical sizes of these galaxies are independent or only mildly dependent on the wavelength, within the errors. The presence of an active nucleus is suspected in two out of six galaxies (33%), opening the intriguing possibility that a large, presently unaccounted population of AGN is hosted in these galaxies, possibly responsible for the cessation of star formation.

Subject headings: cosmology: observations — galaxies: fundamental parameters — galaxies: evolution

1. INTRODUCTION

Most of the stellar mass observed in today's early–type galaxies has assembled at high redshifts ($z > 2$, see Renzini 2006). Thus, the evolution of the mass functions and morphology of these galaxies is expected to provide information on the mechanisms that have assembled and shaped them in their current state, e.g. merging and accretion.

Recent works agree that the most massive early–type galaxies (with $M/M_\odot > 10^{11}$) were already in place at z$\sim$ 1, and characterized by a mass–dependent evolution of the luminosity function, wherein galaxies with lower mass evolve faster (Thomas et al. 2005; Franceschini et al. 2006, Bundy et al. 2006, Scarlata et al. 2007).

Galaxies at $1.5 < z < 3$ with stellar mass and SEDs similar to those of local early types have also been identified and studied (e.g. Franx et al. 2003; Daddi et al. 2004; Kong et al. 2006; Ilbert et al. 2009; McCracken et al. 2009, Cimatti et al. 2008; Kriek et al. 2008). These galaxies have photometrically–measured stellar mass $m \sim 10^{11}$ M$_\odot$ and specific star formation rate SSFR$< 10^{-2}$ Gyr^{-1}, nearly one order of magnitude lower than that of the Milky Way. There is broad agreement that the number density of these high–redshift "elliptical galaxies" rapidly increases from z$\sim$ 2 to z$\sim$ 1 (Fontana et al. 2006; Arnouts et al. 2007; Ilbert et al. 2009). The mechanisms through which they build up their mass, however, are not yet known. Especially intriguing is the recent discovery that at least some massive elliptical galaxies at $z > 1.5$ are, on average, $\sim 3\times$ smaller, and thus $\approx 30\times$ denser, than their local counterparts (Daddi et al. 2005; Trujillo et al. 2006; Trujillo et al. 2007; Toft et al. 2007; Zirm et al. 2007; Longhetti et al. 2007; Cimatti et al. 2008, Van Dokkum et. al. 2008, Buitrago et al. 2008, Toft et al. 2009), a fact lacks an explanation in terms of evolutionary mechanisms (e.g. Hopkins et al. 2009a). Recent works (Valentinuzzi et al. 2009; Trujillo et al. 2009), reported the identification of similarly dense massive galaxies in the local universe, although their spatial density seems smaller than the $z \sim 2$ galaxies.

Some have suggested that current observations at high redshift could have missed low surface-brightness halos surrounding these galaxies, due to the relatively limited sensitivity of current imaging data (Hopkins et al. 2009b; Mancini et al. 2009). If true, this could help explain the apparently dramatic morphological transformation of passive galaxies from $z \sim 2$ to the present. Another possibility is that current surveys of the local universe

[1] Based on data obtained with the *Hubble Space Telescope* operated by AURA, Inc. for NASA under contract NAS5-26555.

[2] Department of Astronomy, University of Massachusetts, Amherst, MA 01003; paolo@astro.umass.edu

[3] Space Telescope Science Institute, 3700 San Martin Boulevard, Naltimore, MD, 21218

[4] Osservatorio Astronomico di Padova (INAF-OAPD), Vicolo dell'Osservatorio 5, I-35122, Padova, Italy

[5] INAF - Osservatorio Astronomico di Roma, via Frascati 33, Monteporzio-Catone (Roma), I-00040, Italy

[6] NOAO-Tucson, 950 North Cherry Avenue, Tucson, AZ 85719

[7] University of Nottingham, School of Physics and Astronomy, Nottingham NG7 2RD

[8] George P. and Cynthia Woods Mitchell Institute for Fundamental Physics and Astronomy, Department of Physics, Texas A&M University, College Station, TX 77843-4242, USA

[9] Astrophysics Science Division, Observational Cosmology Laboratory, Goddard Space Flight Center, Code 665, Greenbelt, MD 20771

[10] Jet Propulsion Laboratory, California Institute of Technology, MS 169-327, Pasadena, CA 91109

(e.g. the SDSS, Stoughton et al. 2002) could also have missed a relatively large fraction of very compact, early–type galaxies due to the limited ground–based angular resolution (1 arcsec corresponds to a physical scale of ~ 1 kpc at $z = 0.05$).

A crucial step is to obtain an unbiased and statistically accurate measure of the size distribution of early–type galaxies at both high and low redshift (Cassata et al. in prep.). So far, while small high–redshift samples have been imaged with NICMOS at rest–frame optical wavelengths (Trujillo et al. 2007; Toft et al. 2007; Zirm et al. 2007; Longhetti et al. 2007; Van Dokkum et. al. 2008), most of the galaxies only have rest–frame UV images from ACS and the dependence of the morphology of these galaxies on the wavelength has not been characterized (Cimatti et al. 2008; Daddi et al. 2005).

In this letter we use the unprecedented sensitivity and angular resolution of WFC3/IR images recently acquired in the HUDF to study the optical rest–frame morphology, as well as the spectral energy distributions, of a small but well defined sample of low SSFR galaxies at z$\sim$2. The WFC3 images, in the Y–, J– and H–bands (F105W, F125W and F160W, respectively) have PSF with FWHM=0.18" at 16000Å) and reach $1-\sigma$ surface brightness fluctuations of 27.2, 26.6 and 26.3 AB/arcsec^2, respectively, the sharpest and deepest ever obtained to date.

2. DATA ANALYSIS

The data consist of the first epoch of WFC3/IR observations acquired by Bouwens et al. (2009, program ID=GO11563, P.I. G. Illingworth) in the HUDF (Beckwith et al. 2006), a $\approx 3.3 \times 3.3$ arcmin^2 field fully embedded in the GOODS–South field (Giavalisco et al. 2004) and imaged with the same photometric system, i.e. the ACS BViz. This first epoch of data covers an area roughly equal to the footprint of the WFC3/IR camera (2.1 arcmin^2) and consists of images in the F105 (Y), F125W (J) and F160W (H) filters. We have carried out our independent reduction of the raw data and after rejecting images affected by persistence in the J–band, our final stacks reach $1-\sigma$ surface brightness fluctuations of 27.2, 26.6 and 26.3 in the three bands, respectively. The WFC3 images have been drizzled to a 0.06" pixel scale.

We selected a sample of high redshift (z$>$ 1.3) passive (SSFR$< 10^{-2} Gyr^{-1}$) and massive (M$> 10^{10} M/M_{\odot}$) galaxies from the GOODS multi–band GUTFIT photometric catalog by Grogin et al. (in preparation). This catalog contains matched photometry for all the photometric bands used for the GOODS multi-facility program from the U to the 8μm IRAC band (the MIPS 24μm photometry is not included). All our sample galaxies have no detection at 24μm down to a $1-\sigma$ limit of 5μJy. Fontana et al. (2009) have shown that it is possible to select a sample of passive galaxies at high-z combining MIPS 24μm to the optical-NIR spectral energy distribution. We used both the BzK color–selection criteria for passive galaxies by Daddi et al. (2004), as well as multi–band SED fitting to identify the sample. While the BzK technique provides a well characterized criterion to select galaxies with low specific star–formation rate (dubbed "pBzK", or passive BzK), the method naturally has finite completeness and contamination, since photometric errors and the intrinsic dispersion of galaxies' broad–band UV/Optical SED scatter galaxies out of the selection window and interlopers into it. Thus, given the overall limited size of the sample, we have augmented it with galaxies selected for being massive and passive according to the above criteria based on fitting their observed broad–band GUTFIT SED to stellar population synthesis models. We used both the Charlot & Bruzual (2007) and Maraston (2005) models with Salpeter IMF and lower and upper mass limits 0.1 and 100 $M_{\odot}$, respectively, obtaining similar results with both libraries.We also use the Calzetti et al. (2000) obscuration law to account for the possible (modest) presence of dust and the Madau (1995) cosmic opacity. The results of the SED fitting are reported in Table 1, and the SEDs are shown in Fig. 1.

The final sample, summarized in Table 1, consists of six galaxies, four of which have spectroscopic redshifts, i.e. 22704 and 23555 from Cimatti et al. (2008), 24279 from Daddi et al. (2005) and 24626 from Vanzella et al. (2008), and two for which we derived accurate ($\Delta z/(1+z) \sim 0.05$) photometric redshifts from the GUTFIT multi-band photometry. Four out of six galaxies satisfy the pBzK criterion.

We have used GALFIT (Peng et al. 2002) to fit the light profile of the galaxies in the z–, Y–, J– and H–bands to the Sérsic model

$$I(r) = I_e exp\left\{-b_n\left[\left(\frac{r}{r_e}\right)^{1/n} - 1\right]\right\}, \qquad (1)$$

where $I(r)$ is the surface brightness measured at distance r, I_e is the surface brightness at the effective radius r_e and b_n is a parameter related to the Sérsic index n. For n=1 and n=4 the Sérsic profile reduces respectively to an exponential or deVaucouleurs profile. Bulge dominated objects typically have high n values (e.g. $n > 2$) and disk dominated objects having n around unity. Cassata et al. (2005), Ravindranath et al. (2006) and Cimatti et al. (2008) showed that this method gives basically unbiased estimates of the Sérsic index and effective radius.

The PSF used by GALFIT to convolve the model has been obtained averaging six bright unsaturated stars in the UDF/WFC3 field. GALFIT has been run considering the sky as a free parameter and using a fitting region around each galaxy of 6×6 arcsec^2. We have run tests using a different region size and fixing the sky to different values, and the Sérsic indices and sizes so obtained were in agreement with the fiducial values within 20%.

3. THE MORPHOLOGICAL PROPERTIES OF GALAXIES AT $Z \sim 2$.

Figure 1 shows for each galaxy the $H-$band images, together with the SED best–fit models, and Figure 2 shows the residuals after subtracting from the galaxies the GALFIT best–fit models, together with the galaxy and model profiles. Even on visual inspection, all the galaxies except 24646 appear to be very compact and relatively symmetric, in close resemblance to present–day spheroidal galaxies. The only exception is galaxy 24626, the most extended of our sample, whose isophotes deviate from an elliptical one, with the position angle varying for different isophote levels. These irregularities can be the result of ongoing or recent interactions.

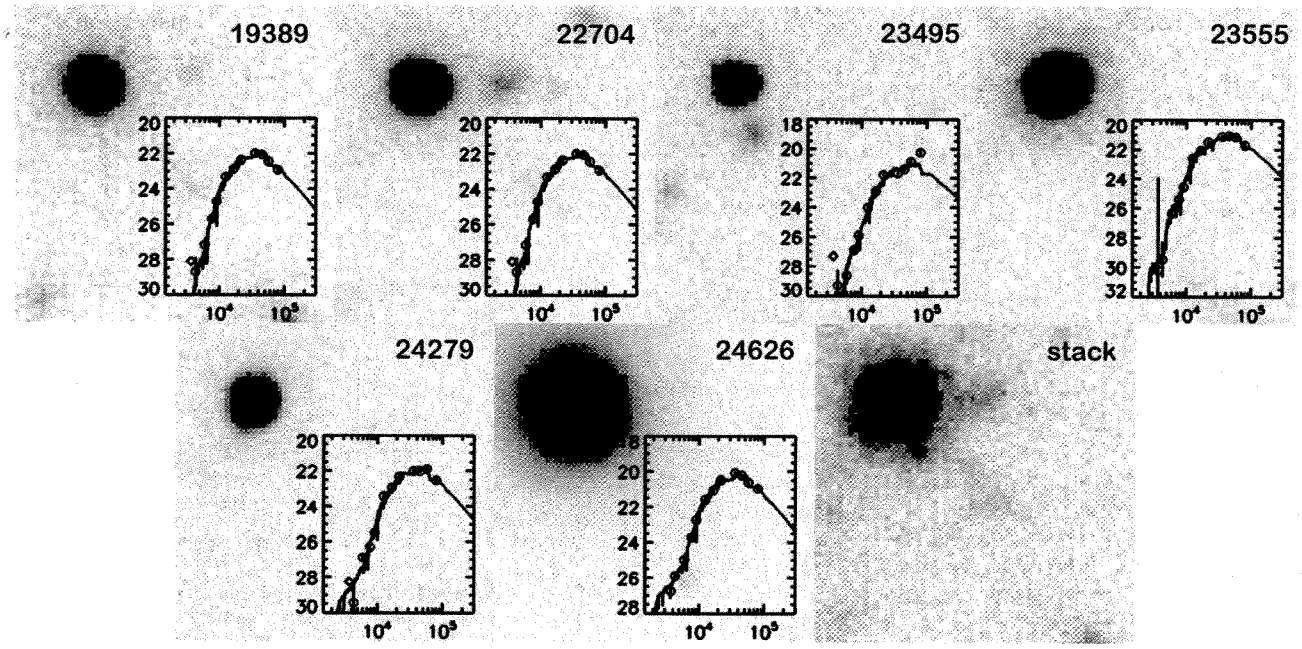

FIG. 1.— For the six galaxy in the sample, and for the stack of the five compact ones (19389, 22704, 23495, 23555, 24279), we show the image in the H–band. The panels are $\sim 3.5 \times 3.5 arcsec^2$. The insets report the SEDs with the photometric best-fit models.

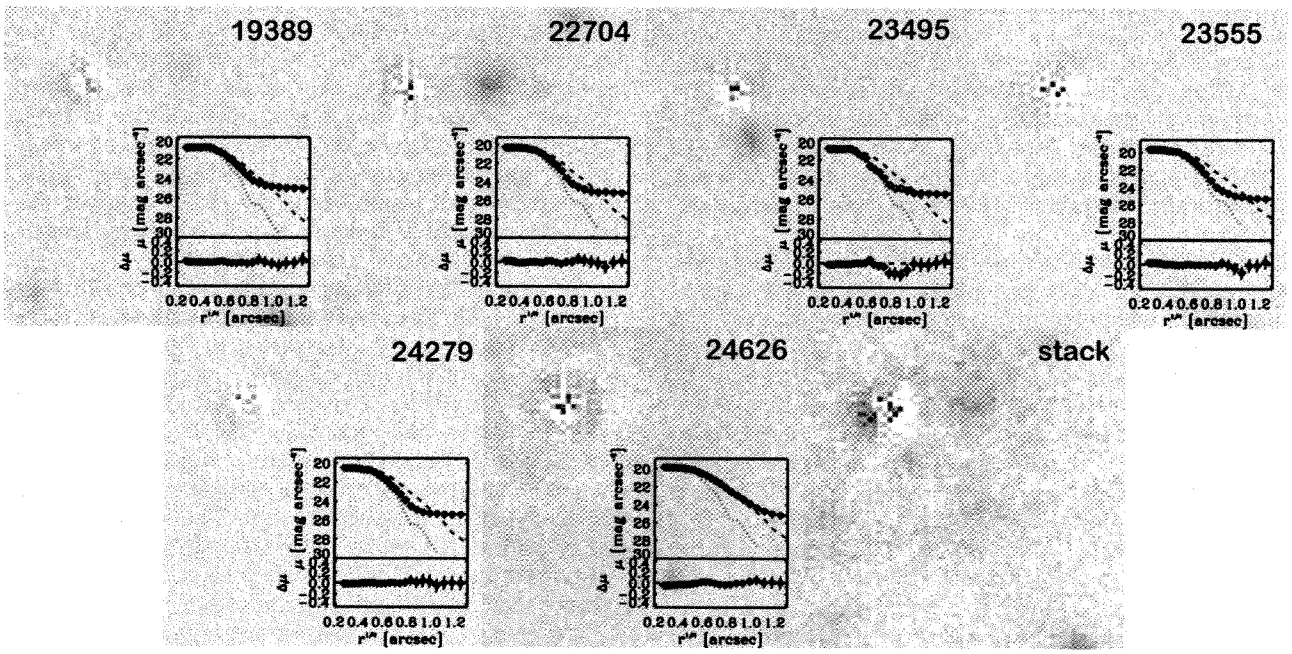

FIG. 2.— For the six galaxy in the sample, and for the stack of the five compact ones, we show the residuals after subtracting the best-fit models. The insets show the galaxy profiles (diamonds), the best-fit profiles (continuous line), the psf profile (dotted line), a Sérsic model with $r_e = 3kpc$ and $n_{Sersic} = 4$ (dashed line) and the residual profile (bottom panel).

The GALFIT Sérsic indices and sizes from the H–band images are listed in Table 1; they quantitatively validate the conclusions derived from the visual inspection. Of the six galaxies, four have Sérsic index $\gtrsim$2 (19389, 22704, 23555 and 24626). In the case of object 19389 we had to add a central unresolved (PSF) component to the Sérsic model to obtain a reasonable fit. This central stellar object contains less than 10% of the total light in the object, and may be indicative of an AGN. This galaxy however is not detected in the Chandra Deep Field South 2-Megasecond Catalog (Luo et al. 2008). Galaxy 23495 also has a peculiar morphology: based on the FWHM, the object is barely resolved in all bands, Fig. 2 shows that the inner part of the galaxy's profile (r$\lesssim$ 1 arcsec) follows quite well the PSF profile, while the GALFIT best fit is that of an unresolved (PSF) light profile, again suggesting the presence of an AGN. Object 23495 is indeed detected in the Chandra images and has luminosity $3.2{\times}10^{43} erg/s$ and $4.8{\times}10^{43} erg/s$ in the soft and hard band, respectively. Object 24279 has a Sérsic index of in-

TABLE 1
THE SAMPLE OF PASSIVE GALAXIES

ID	z[1]	$\log(M/M_\odot)$	log(SSFR) [Gyr^{-1}]	Sérsic $H-$band	r_e [kpc]
19389	1.307p	10.41	-5.55	2.99 [2]	1.02 [2]
22704	1.384s	10.70	-5.55	2.65	0.50
23495	2.349p	11.14	-3.39	[3]	< 0.38
23555	1.921s	10.82	-2.98	1.97	0.44
24279	1.980s	10.63	-3.39	1.63	0.37
24626	1.317s	11.10	-2.11	7.42	3.69

NOTE. — (1): *s* and *p* indicate respectively spectroscopic and photometric redshifts; (2) the morphology of this object is reproduced by adding to the Sérsic model a central psf component; (3) the morphology of this object is reproduced by a single central psf component, so the size reported here is just an upper limit.

termediate value n∼1.6, suggesting that this is probably a bulge dominated disk galaxy. Finally, to obtain a reasonable fit to object 24626, we had to use a combination of two components: one Sérsic model with a very high Sérsic index to reproduce the inner part of the galaxy, and a second one with n∼1 to reproduce the outskirts.

It is also interesting to analyze the residual maps produced by subtracting the best–fit model from the original image to investigate the presence of diffuse low–surface brightness halos, as recently suggested by some (Mancini et al. 2009; Hopkins et al. 2009b). The residual maps in Fig. 2 show some residual noise in the inner 0.5": this is because we are using an averaged PSF, but the actual PSF is slightly asymmetric and not homogeneous across the field. As a test, we fitted the individual stars using the composite PSF used for galaxies, and we find similar residuals. Moreover, the residual profiles in the bottom panels of Fig. 2 do not show any significant deviation from the model in the inner part of the galaxies.

No diffuse halo is observed once the best fit solution is subtracted. The only exception could be the case of galaxy 24626, which requires a two–component model to reproduce its light profile, possibly an inner bulge and an outer disk. Subtracting both of these two components, however, leaves a complex residual map, revealing a substantially more irregular light distribution compared to the other galaxies. Finally, note that both components have effective radius r_e ∼3 kpc, implying that even if observed in shallower images that miss the low surface brightness component, the effective radius would still be found to be ∼ 3 kpc, significantly more diffuse than the other galaxies.

To further explore the possible presence of a faint halo around these galaxies we have stacked together all of them except galaxy 24626 and then fitted the stacked image with GALFIT following the same procedure used for individual galaxies. The stacked image, which also looks very compact, is shown in Fig. 1, and the GALFIT residual map in Fig. 2. The residual image, consistent with what we have found analyzing the individual galaxies, does not show any large–scale diffuse halo (close companions have not been masked before the stack and have not been fitted). For all the galaxies and for the stacked image the amount of residual light in the inner 2" is lower than 2% of the total light in the galaxy within the same aperture.

In Figure 3 we compare the Sérsic profiles in the z, Y, J and H bands, sampling the morphology from the rest–

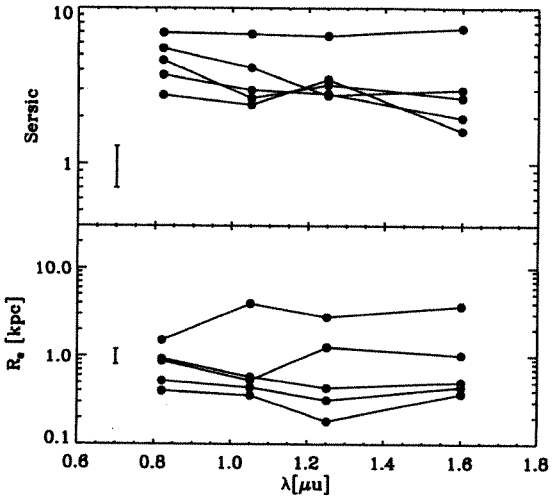

FIG. 3.— For the 5 galaxies in the sample best fitted by a Sérsic model, we show the Sérsic index (*upper panel*) and the effective radius (*bottom panel*) as a function of the wavelength. Object 23495, that is best-fitted by a point like source, is not reported in this figure. The typical error bars are shown, and amount to about 30% on the Sérsic indices and to about 20% on sizes.

frame UV at $\lambda \sim 3300$ Å to the optical one at ~ 6000 Å (assuming mean redshift $< z >= 1.7$). Consistent with our visual inspection, this shows weak or no evidence of morphological k-correction, since the Sérsic index only slightly decreases from the z through the H band, implying only a slighty higher more compact morphology at bluer wavelengths than at redder ones. This is in agreement with reports that the morphology of elliptical galaxies is largely independent of the wavelength (Papovich et al. 2003; Cassata et al. 2005).

Similarly, the effective radius of all the six galaxies in our sample does not depend on the wavelength (see bottom panel of Fig. 3), with two of them showing no dependence of the size on the wavelength within the errors, and three showing a slight, but statistically significant, decrease with increasing wavelengths, being ∼ 40% smaller in H band than in the z one. This results in a negative color gradient, with the outer part of the galaxies being bluer than the center. This color gradient has also been measured by Guo et al. (in preparation) using aperture photometry, and they report that SED fitting shows that the stellar populations in the outer parts of these passive galaxies are, on average, ∼ 0.5 Gyr younger than those in the center. We note that the mild dependence of the morphology of our galaxies on wavelength is in good agreement with other studies of early–type galaxies at high–redshift from ACS and NICMOS images (McCarthy et al. 2007; Trujillo et al. 2007).

4. THE MASS-SIZE RELATION AT $Z \sim 2$

In Figure 4 we compare the relationship between mass and size (in the H band) for the six galaxies in our sample to other measures and to local galaxies (see figure caption). The mass measurements have been homogenized to CB07 and Salpeter IMF, applying typical offsets: we used $M_{CB07} = M_{BC03} - 0.2$ and $M_{Salp} = M_{Chab} + 0.25$ (Salimbeni et al. 2009). Four out of our six galaxies are located below the local relation for early–type galaxies,

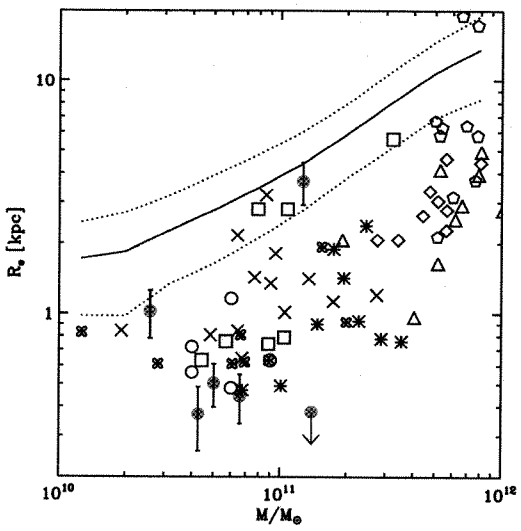

FIG. 4.— The distribution of effective radii versus stellar mass for galaxies in our sample (red filled circles). The continuous and dashed lines represent the local relation and its scatter, from Shen et al. (2003). Galaxy 23495 is shown as an upper limit, since its best-fit is a stellar-like profile. Crosses, circles, clovers, squares, stars, triangles, pentagons and diamonds indicate the early-types of Cimatti et al. (2008), Zirm et al. (2007), Toft et al. (2007), Daddi et al. (2005), Van Dokkum et al. (2008), Trujillo et al. (2006), Mancini et al. (2009) and Longhetti et al. (2007). Mass measurements have been homogenized to CB07 models and Salpeter IMF.

in agreement with other repoirts that massive galaxies at $z \sim 2$ are significantly more compact than their local counterparts. The remaining two (19389, the object with a stellar component at the center, and 24626, the large elliptical with multiple components) are on the local relation. We find it intriguing that these two galaxies also are the ones with the lowest redshift in our sample.

Thus, the sample that we have discussed here confirms the existence of very compact and dense passive galaxies at $\sim$ 2, on average about 3 to 5 times smaller and about 50–100 times denser than local counterparts, reported by other authors from similar but shallower and/or lower quality images (Trujillo et al. 2007; Toft et al. 2007; Zirm et al. 2007; Longhetti et al. 2007; Van Dokkum et al. 2008; Toft et al. 2009) or at UV rest-frame wavelengths (Daddi et al. 2005; Cimatti et al. 2008). It, however, also suggests a diversity of morphological properties (size and stellar mass density) among these galaxies, with some of them, possibly the ones detected at lower redshifts (i.e. $1.3 < z < 1.5$) being rather similar to those observed in the local universe.

5. SUMMARY AND CONCLUSIONS

We have studied the UV and optical rest–frame morphology of 6 passively evolving galaxies $1.3 < z < 2.4$, four of which have spectroscopically confirmed redshifts.

Based on visual inspection and on the analysis of the azimuthally averaged light profile, which is well described by a Sérsic profile, we classify the morphology of our six galaxies as "elliptical". This is consistent with their elary–type spectral energy distribution, suggesting a tight correlation between spectral and morphological properties in close similarity to what is observed in the local universe, i.e. the Hubble sequence. Two of our six galaxies (33% of the sample) appear to have a spatially unresolved nuclear component consistent with an AGN. One of these two galaxy, object 23495, is actually detected in the 2–MS Chandra images and has $L_X \sim 3.5 \times 10^{43} erg/s$; the central point source is also responsible for the $\gtrsim$ 90% of the observed luminosity in the H–band. The colors of this putative nuclear component are as red as those of the rest of the galaxy. While our sample is undoubtly small, this apparently high incidence of faint and red AGN in galaxies with very low specific star formation rates at $z \sim 2$, the cosmic era when AGN activity reaches its maximum (Ueda et al. 2003, Hasinger et al. 2005), raises the intriguing question of whether we have finally found evidence that nuclear activity is directly responsible for terminating star formation in massive galaxies. High–resolution imaging at UV and optical rest–frame wavelengths seems to be very efficient in finding this faint and red nuclear sources (only one out of two is detected by Chandra), suggesting that a large imaging survey with WFC3 might provide an efficient methodology to study this problem.

Overall the Sérsic analysis yields similar results regardless of the bandpass indicating that for these galaxies the morphological k–correction between the rest–frame UV and optical is small. This particular property opens the possibility to study the morphology of these galaxies using large, deep and well–controlled samples available from the optical images of the GOODS and other similar surveys. We plan to report on such studies in a forthcoming paper (Cassata et al. in preparation), where we compare the distribution of mid–UV morphology of $\sim$150 passive galaxies at $z \sim 2$ from GOODS (z–band) with those of local early–type galaxies from the SDSS at the same rest–frame wavelength (u–band).

We do not see any evidence of a faint halo surrounding the compact core of these galaxies, neither in the individual residuals, nor in stacked images, for five out of six galaxies in our sample. One galaxy, object 24626, requires at least two components to provide a good fit, one Sérsic model with high n (spheroid) embedded in a low surface brightness disk.

Four out of six galaxies in our sample lie below the local mass–size relation for early–type galaxies, confirming previous reports that such galaxies at $z\sim$ 2 can be $\sim$ 3 times more compact at a given mass and thus $\sim$ 50 times denser than locally. One of our galaxies, however (object 19389), which has an unresolved central component, is on the boundary of the local relation, while another (object 24626) is well within the local relation. Thus, the deep WFC3 images also show, as suggested in other previous studies (Cimatti et al. 2008; Mancini et al. 2009) that there are early–type galaxies at $z > 1.5$ with size and mass similar to those of local counterparts.

REFERENCES

Arnouts, S. et al. 2007, A&A, 476, 137
Beckwith, S. V. W. et al. 2006, AJ, 132, 1729
Buitrago, F., et al. 2008, ApJ, 687, 61L
Bundy, K., et al. 2006, ApJ, 651, 120
Calzetti, D., et al. 2000, ApJ, 533, 682
Cassata, P., et al. 2005, A&A, 357, 903

Cimatti, A., et al. 2008, A&A, 482, 21
Daddi, E., et al. 2004, ApJ, 617, 746
Daddi, E., et al. 2005, ApJ, 626, 680
Fontana, A., et al. 2006, A&A, 459, 745
Fontana, A., et al. 2009, A&A, 501, 15
Franceschini, A., et al. 2006, A&A, 453, 397
Franx, M., et al. 2003, ApJ, 587, 79
Giavalisco, M., et al. 2004, ApJ, 600, L93
Hasinger, G., Miyaji, T., Schmidt, M. 2004, A&A 441, 417
Hopkins, P. F., et al. 2009, [astro-ph/0909-2039]
Hopkins, P. F., et al. 2009, MNRAS, 398, 898
Ilbert, O., et al. 2009, [astro-ph/0903-0102]
Longhetti, M., et al. 2007, MNRAS, 374, 614
Luo, B., et al. 2008, ApJS, 179, 19
Kong, X., et al. 2006, ApJ, 638, 72
Kriek, M., et al. 2007, ApJ, 677, 219
Maraston, C., 2005, MNRAS, 362, 799
McCracken, H. J., et al. 2009, [astro-ph/0910-2705]
Mancini, C., et al. 2009, [astro-ph/0909-3088]
Madau, P., 1995, ApJ, 441, 18
Papovich, C., et al. 2003, ApJ, 598, 827
Peng, C. Y., et al. 2002, AJ, 124, 266
Renzini, A., 2006, ARA&A, 44, 141
Salimbeni, S., et al. 2009, American Institute of Physics Conference Series, Vol. 1111, 207
Scarlata, C., et al. 2007, ApJS, 172, 494
Shen, S., et al. 2003, MNRAS, 343, 978
Stoughton, C., et al. 2002, AJ, 123, 485
Thomas, D., et al. 2005, ApJ, 621, 673
Toft, S., et al. 2007, ApJ, 671, 285
Toft, S., et al. 2009, ApJ, 705, 255
Trujillo, I., et al. 2006, MNRAS, 373, L36
Trujillo, I., et al. 2007, MNRAS, 382, 109
Ueda, Y., et al. 2003, ApJ, 598, 886
Van Dokkum, P. G., et al. 2008, ApJ, 677, L5
Valentinuzzi, T., et al. 2009, [astro-ph/0907-2392]
Vanzella, E., et al. 2008, A&A, 478, 83
Zirm, A. W., et al. 2007, ApJ, 656, 66